

Heavy-quark mass effects in off-light-cone distributions

Valerio Bertone^a, Michael Fucilla^b, Cédric Mezrag^a

^a*Irfu, CEA, Université Paris-Saclay, Gif-sur-Yvette, F-91191, France*

^b*Université Paris-Saclay CNRS/IN2P3, IJCLab, Orsay, F-91405, France*

Abstract

We compute the one-loop correction to the forward matrix element of an off-light-cone bi-local quark correlator characterised by a space-like separation z^2 in the presence of heavy quarks with mass m . This calculation allows us to extract the one-loop matching kernel, necessary to connect quasi and pseudo-distributions to collinear parton distribution functions (PDFs), accounting for heavy-quark mass effects. Our result is exact in that it includes all powers of $z^2 m^2$ at one loop in α_s . In the limit $z^2 m^2 \rightarrow 0$, it consistently reduces to the known massless result. We also carry out an implementation of our expression, which allows us to compute the charm pseudo-distribution of the proton given its PDF. We finally comment on the quantitative impact of heavy-quark mass corrections.

Keywords: Hadron structure, Lattice QCD, Pseudo-distributions, Quasi-distributions

1. Introduction

In the past decades, much effort has been put into attempting to extract information on the structure of hadrons from lattice simulations of Quantum Chromodynamics (QCD) (see *e.g.* the reviews in Refs. [1–3]). However, the task is complicated by the fact that most of the phenomenologically relevant partonic distributions are defined through bi-local partonic operators characterised by light-like separations. Typical examples are parton distribution functions (PDFs) and distribution amplitudes (DAs).

Because of the use of euclidean metric, light-like distances in lattice-QCD simulations are reduced to a point, limiting the studies to local operators related to moments of the distributions of interest. Moreover, the breaking of Lorentz symmetry generates complicated mixings between operators, effectively restricting the computation to the lowest moments. In spite of early attempts to overcome this issue [4–6], the breakthrough came in 2013 with Ref. [7], introducing the Large-Momentum Effective Theory (LaMET) formalism, which for the first time gave direct access to the momentum dependence of light-cone distributions. The new formalism was shortly followed by the so-called short-distance factorisation approach [8], which allows for a simpler connection between lattice simulations and momentum dependence of light-cone distributions. Other formalisms have also been developed (see, *e.g.*, Refs. [9–12]).

In both LaMET and short-distance factorisation, off-light-cone distributions are related to light-cone distributions by means of perturbative matching kernels. It is precisely these relations that allow light-cone distributions, such as PDFs and DAs, to be extracted from lattice simulations. Currently, LaMET matching kernels for PDFs are known up to next-to-next-to leading order [13–19], *i.e.* $\mathcal{O}(\alpha_s^2)$ in the QCD strong coupling. In the short-distance-factorisation formalism, instead, they are available up to one loop [8, 20–26], *i.e.* $\mathcal{O}(\alpha_s)$. Furthermore, several efforts have also been de-

voted to the calculation of higher-twist contributions to off-light-cone distributions [27–32]. As a demonstration of the relevance of these quantities, a significant number of studies have recently emerged which make use of these kernels (see, *e.g.*, Refs. [33, 34] for recent lattice QCD extractions of GPDs), along with first attempts to improve our knowledge of hadron structure incorporating both experimental and simulated data [35–37].

Motivated by recent lattice extractions of heavy-meson DAs and PDFs [38–40], in this paper we set out to incorporate heavy-quark mass effects into the computation of the matching kernels. Specifically, our purpose is to evaluate power corrections of $z^2 m^2$ to the partonic non-singlet distribution with space-like separation z^2 in forward kinematics (a.k.a. pseudo-distribution) of a heavy quark with mass m up to one-loop accuracy. This calculation will eventually allow us to extract the matching kernel to connect the heavy-quark non-singlet pseudo-distribution to the corresponding PDF. In this paper, we present the main steps of the calculation, highlighting its main properties and checking its consistency with past results. We leave to a future publication the study of mass effects in the singlet sector, as well as a more detailed discussion on technical aspects. Here, we limit ourselves to observing that pseudo-distributions are intimately related to transverse-momentum dependent distributions (TMDs). This connection allows us to leverage past results to achieve a full description of non-singlet and singlet sectors at one loop including heavy-quark mass corrections (see, *e.g.*, Refs. [41, 42])

The paper is organised as follows. In section 2, the basic notation is introduced. In section 3, the calculation of the one-loop massive pseudo-distribution is described. In section 4, the massive matching kernel is finally extracted. A numerical estimate of heavy-quark mass effects is presented in section 5. Finally, in section 6 we give a summary, draw our conclusions, and present an outlook.

2. Ioffe-time distribution

Let us start by consider the QCD quark string operator

$$O^\alpha = \bar{\psi}(0)\gamma^\alpha W(0, z, A)\psi(z), \quad (1)$$

where

$$W(0, z, A) = \mathcal{P}\exp\left[igz_\nu \int_0^1 dt \hat{A}^\nu(tz)\right] \quad (2)$$

is a straight-line gauge link in the fundamental representation. In Ref. [21], it has been shown that the matching kernel can be computed directly at the operator level in the Balitsky-Braun spirit [43]. However, since the massive computation is particularly involved, we work at the level of the distribution and compute the perturbative kernel using a target quark. We thus consider the Ioffe-time distribution of a quark, which reads

$$\mathcal{M}^\alpha(\nu, z^2) = \frac{1}{2N_c} \sum_{c,\lambda} \langle p, \lambda | \bar{\psi}(0)\gamma^\alpha W(0, z, A)\psi(z) | p, \lambda \rangle, \quad (3)$$

where the sum is over colour and quark helicities, and $\nu = -p \cdot z$ is the Ioffe time, p being the quark momentum. The Ioffe-time distribution can be parametrised as

$$\mathcal{M}^\alpha(\nu, z^2) = 2p^\alpha f(\nu, z^2) + z^\alpha \tilde{f}(\nu, z^2). \quad (4)$$

We consider the space-like separations, through the equal-time parametrisation $z = (0, 0, 0, z^3)$, and the $\alpha = 0$ component, which allows one to avoid higher-twist contaminations in lattice calculations.

At the leading order, the Wilson line is equal to the identity in colour space and thus we have:

$$\mathcal{M}^0(\nu) = \frac{1}{2N_c} \sum_{c,\lambda} \langle p, \lambda | \bar{\psi}(0)\gamma^0\psi(z) | p, \lambda \rangle = 2p^0 e^{i\nu} \equiv 2p^0 f(\nu). \quad (5)$$

The fourier transform of $f(\nu)$ immediately gives the leading-order quark parton distribution function (PDF)

$$f(x) = \frac{1}{2\pi} \int_{-\infty}^{+\infty} d\nu e^{-i\nu x} f(\nu) = \delta(1-x). \quad (6)$$

In what follows, we extensively use the plus-prescription distribution defined as

$$\int_0^1 d\beta [f(\beta)]_+ g(\beta) = \int_0^1 d\beta f(\beta) [g(\beta) - g(1)], \quad (7)$$

where $f(\beta) \sim 1/(1-\beta)$ around $\beta = 1$ while $g(\beta)$ is a regular function. Ultraviolet (UV) divergences are always regularised in dimensional regularisation in $D = 4 - 2\epsilon_{UV}$ dimensions. Infrared (IR) divergences are instead absent due to the non-vanishing quark mass m .

3. One-loop calculation

3.1. Wilson-line self-energy contribution

We work in Feynman gauge and thus we get a contribution from the Wilson-line self-energy in fig. 1. This contribution

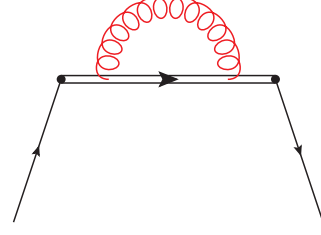


Figure 1: Wilson-line self-energy contribution.

vanishes on the light-cone, where $z^2 = 0$, and is independent from the mass. It can be obtained directly at the operator level by perturbatively expanding the Wilson line at the second order in eq. (1), *i.e.*

$$\begin{aligned} O_{\text{Wils.}}^\alpha &= \bar{\psi}(0)\gamma^\alpha \frac{(ig)^2}{2} z^\mu z^\nu \\ &\times \int_0^1 dt_1 \int_0^1 dt_2 \left[\theta(t_1 - t_2) (t^\alpha t^\beta)_{ij} \overline{A_\mu^a(t_1 z)} A_\nu^b(t_2 z) \right. \\ &\left. + \theta(t_2 - t_1) (t^\beta t^\alpha)_{ij} \overline{A_\nu^b(t_2 z)} A_\mu^a(t_1 z) \right] \psi(z). \end{aligned} \quad (8)$$

It is easy to show that

$$\begin{aligned} O_{\text{Wils.}}^\alpha &= (ig)^2 \frac{C_F}{2} \int_0^1 dt_1 \int_0^1 dt_2 z^\mu z^\nu D_{\mu\nu}(z(t_1 - t_2)) \bar{\psi}(0)\gamma^\alpha\psi(z) \\ &\equiv \Gamma_W(z) \bar{\psi}(0)\gamma^\alpha\psi(z), \end{aligned} \quad (9)$$

where $D_{\mu\nu}$ is gluon propagator in position space, which in dimensional regularisation reads

$$D_{\mu\nu}(y) = -\frac{g_{\mu\nu}\Gamma(D/2 - 1)}{4\pi^{D/2}(-y^2 + i0)^{D/2-1}}. \quad (10)$$

Using the explicit form of the propagator, we immediately get

$$\begin{aligned} \Gamma_{\text{Wils.}}(z) &= -\frac{g^2 C_F}{8\pi^{D/2}} \Gamma\left(\frac{D}{2} - 1\right) \\ &\times (-z^2) \int_0^1 dt_1 \int_0^1 dt_2 \frac{1}{[-z^2(t_1 - t_2)^2]^{D/2-1}}. \end{aligned} \quad (11)$$

In $D = 4$, the integral is divergent. There are several possible ways to regularise it. In the seminal paper [21], these divergences were analysed using the Polyakov prescription

$$\frac{1}{[-z^2(t_1 - t_2)^2]} \rightarrow \frac{1}{[-z^2(t_1 - t_2)^2 + a^2]}. \quad (12)$$

Besides standard logarithmic singularities, this prescription leads to linear divergences that are interpreted as the renormalisation of a mass moving along the gauge link. We do not delve into such complications and use the more pragmatic dimensional regularisation. Then, it is easy to see that

$$\begin{aligned} \Gamma_{\text{Wils.}}(z) &= -\frac{g^2 C_F}{8\pi^{D/2}} \Gamma\left(\frac{D}{2} - 1\right) (-z^2)^{2-D/2} \\ &\times \int_0^1 dt_1 \int_0^1 dt_2 \frac{1}{[(t_1 - t_2)^2]^{D/2-1}}. \end{aligned} \quad (13)$$

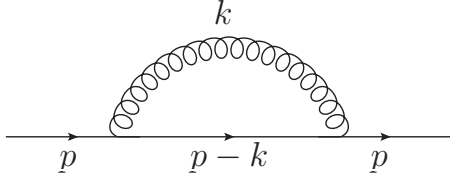


Figure 2: One-loop quark self energy.

The integral over t_1 and t_2 gives

$$\int_0^1 dt_1 \int_0^1 dt_2 (t_1 - t_2)^{2-D} = 2 \int_0^1 dt_1 \int_0^{t_1} dt_2 (t_1 - t_2)^{2-D} = \frac{2}{(D-3)(D-4)} \quad (14)$$

and we finally get

$$\Gamma_{\text{Wils.}}(z) = -\frac{g^2 C_F}{(4\pi)^{D/2}} \frac{4 \Gamma\left(\frac{D}{2} - 1\right)}{(D-3)(D-4)} \left(\frac{-z^2}{4}\right)^{2-D/2}. \quad (15)$$

This result reproduces that of Ref. [23], apart from the different colour factor (C_F instead of C_A), due to the fact that here we are considering the quark distribution instead of the gluon one. For the one-loop contribution to the Ioffe-time distribution associated to the Wilson-line self-energy, we finally write

$$\mathcal{M}_{\text{Wils.}}(v, z^2) = -\frac{g^2 C_F}{(4\pi)^{D/2}} \frac{4 \Gamma\left(\frac{D}{2} - 1\right)}{(D-3)(D-4)} \left(\frac{-z^2}{4}\right)^{2-D/2} \mathcal{M}^0(v). \quad (16)$$

3.2. Quark-line self-energy contribution

To extract the quark self-energy contribution, we must consider the one-loop quark propagator, which reads

$$i[D_F(p)]_{ij} = \frac{i}{\not{p} - m} \delta_{ij} \times \left[1 + \frac{i(-i\Sigma(p))}{\not{p} - m} + \frac{i[i(Z_2 - 1)\not{p} - i(Z_2 Z_m - 1)m]}{\not{p} - m} \right], \quad (17)$$

where Z_2 and Z_m are the wave-functions and mass renormalisation constants. The factor $(-i\Sigma(p))$ is obtained from the amplitude in fig. 2 by amputating the external spinors, *i.e.*

$$-i\Sigma(p)\delta_{ij} = \int \frac{d^D k}{(2\pi)^D} (-ig\gamma^\mu t_{ik}^a) \frac{i\delta_{kn}}{\not{p} - \not{k} - m} (-ig\gamma^\nu t_{nj}^b) \frac{-i\delta^{ab}}{k^2} g_{\mu\nu}. \quad (18)$$

After some algebra, one obtains

$$\Sigma(p) = \frac{g^2 C_F}{(4\pi)^{D/2}} 2\Gamma\left(2 - \frac{D}{2}\right) \times \int_0^1 d\beta \left[\frac{D}{2} m - \left(\frac{D}{2} - 1\right)(1 - \beta)\not{p} \right] (\beta m^2 - \beta(1 - \beta)p^2)^{\frac{D}{2}-2}. \quad (19)$$

We have to include a correction for each external leg along with a factor of 1/2 as a consequence of the LSZ reduction formula. Moreover, in the presence of the double pole at $\not{p} = m$ in eq. (17), the LSZ theorem prescribes that [44]

$$\Gamma_{\text{Self.}} = \frac{d\Sigma(p)}{d\not{p}} \Big|_{\not{p}=m}. \quad (20)$$

Taking the derivative of right-hand side of eq. (19), we get

$$\Gamma_{\text{Self.}} = -\frac{g^2 C_F}{(4\pi)^{D/2}} (m^2)^{D/2-2} \Gamma\left(2 - \frac{D}{2}\right) \left(3 - 4\left(\frac{D}{2} - 2\right)\right). \quad (21)$$

A first important observation is that the structure of the singularities of the massive self-energy is different from the massless case. It is convenient, in analogy to the massless case [21], to introduce a fictitious dependence on z^2 , by rewriting eq. (21) as

$$\mathcal{M}_{\text{Self.}}(v, z^2, m^2) = \frac{4g^2 C_F}{(4\pi)^{D/2}} \left[(m^2)^{D/2-2} \frac{\Gamma\left(3 - \frac{D}{2}\right)}{D-4} - 1 \right] \mathcal{M}^0(v) + \frac{g^2 C_F}{(4\pi)^{D/2}} \left[\frac{1}{\left(\frac{D}{2} - 2\right)} \left(\frac{-z^2}{4e^{-\gamma_E}}\right)^{2-D/2} + \ln\left(\frac{-z^2 m^2}{4e^{-2\gamma_E}}\right) \right] \times \mathcal{M}^0(v) + \mathcal{O}(D-4), \quad (22)$$

where, in the first line, we have isolated divergences which are absent in the massless computation plus non-logarithmic finite contributions.

3.3. Box-type contribution

The correction to the operator coming from the box-like diagram in fig. 3 reads

$$\mathcal{O}_{\text{Box}}^\alpha = (ig)^2 C_F \int d^D z_1 \int d^D z_2 \times \bar{\psi}(z_2) \gamma_\mu D_F(z_2) \gamma^\alpha D_F(z - z_1) \gamma_\nu \psi(z_1) D^{\mu\nu}(z_2 - z_1). \quad (23)$$

At the level of the quark distribution, we have

$$\mathcal{M}_{\text{Box}}(v, z^2, m^2) = \frac{g^2 C_F \Gamma\left(\frac{D}{2} - 1\right)}{8\pi^{D/2}} \sum_\lambda \int d^D z_1 \int d^D z_2 e^{ip(z_2 - z_1)} \times \frac{\bar{u}_\lambda(p) \gamma_\mu D_F(z_2) \gamma^0 D_F(z - z_1) \gamma^\mu u_\lambda(p)}{[-(z_2 - z_1)^2 + i0]^{D/2-1}}. \quad (24)$$

We use the Fourier representation of the quark propagator

$$D_F(z) = \int \frac{d^D k}{(2\pi)^D} e^{-ikz} \frac{i\not{k}}{k^2 - m^2 + i0}. \quad (25)$$

After performing the shift $z_2 \rightarrow z_2 + z_1$ and integrating over positions by means of the integral

$$\int d^D z \frac{e^{iz(p-k_1)}}{[-z^2/4 + i0]^{D/2-1}} = \frac{i(4\pi)^{D/2}}{\Gamma(D/2 - 1)} \frac{1}{[(k_1 - p)^2 + i0]}, \quad (26)$$

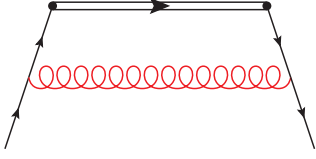


Figure 3: Box-like diagram contribution.

we get

$$\mathcal{M}_{\text{Box}}(\nu, z^2, m^2) = \frac{g^2 C_F}{2} \int \frac{d^D k}{(2\pi)^D i} e^{-ikz} \times \frac{\text{Tr}[(\not{p} + m)\gamma_\mu(\not{k} + m)\gamma^0(\not{k} + m)\gamma^\mu]}{[(k-p)^2 + i0][k^2 - m^2 + i0]^2}. \quad (27)$$

The calculation of the box contribution is lengthy. The general strategy of the computation relies on using the Schwinger representation for the denominators in eq. (27) to integrate over k . For compactness, we only provide the final result and leave the detailed derivation to a future publication [45].

The final result for the box-type contribution reads

$$\begin{aligned} & \mathcal{M}_{\text{Box}}(\nu, z^2, m^2) \\ &= \frac{g^2 C_F}{(4\pi)^{D/2}} \left\{ (m^2)^{D/2-2} \Gamma\left(3 - \frac{D}{2}\right) \left(\frac{-4}{D-4} + 4 \right) \right. \\ & \quad \left. + 2 \left[\frac{1 - \sqrt{-z^2 m^2} K_1(\sqrt{-z^2 m^2})}{-z^2 m^2} \right] \right\} \mathcal{M}^0(\nu) \\ & \quad + \frac{2g^2 C_F}{(4\pi)^{D/2}} \int_0^1 d\beta \left[2(1-\beta) K_0\left(\sqrt{-z^2(1-\beta)^2 m^2}\right) \right]_+ \mathcal{M}^0(\beta\nu) \\ & \quad + \frac{g^2 C_F}{(4\pi)^{D/2}} \int_0^1 d\beta \left[\frac{-4\beta}{1-\beta} \right]_+ \mathcal{M}^0(\beta\nu) \\ & \quad \times \sqrt{-z^2(1-\beta)^2 m^2} K_1\left(\sqrt{-z^2(1-\beta)^2 m^2}\right). \quad (28) \end{aligned}$$

A few comments are in order. First, we observe the presence of mass-generated UV divergences, not present in the massless calculation, which are collected in the second line of eq. (28). As can be seen by comparing eq. (22) to eq. (28), these terms cancel out against analogous terms appearing in the quark self-energy contribution. The term in the third line of eq. (28) emerges as a consequence of the fact that we enforced a plus-prescription structure on the term proportional to $K_0(\sqrt{-z^2(1-\beta)^2 m^2})$. In the massless calculation, this term would cancel the logarithmic one in eq. (22). Indeed, the logarithmic part of the two terms cancels exactly upon expansion around $z^2 m^2 = 0$, if one only retains the leading term (leading-twist expansion). The third term in eq. (28) is dominant in the limit $z^2 m^2 \rightarrow 0$ and, at leading twist, gives a contribution proportional to

$$\ln\left(\frac{4e^{-2\gamma_E}}{-z^2(1-\beta)^2 m^2}\right) = \ln\left(\frac{4e^{-2\gamma_E}}{-z^2}\right) - \ln((1-\beta)^2 m^2). \quad (29)$$

The first term on the r.h.s. of eq. (29) is the so-called z^2 -evolution term characteristic of pseudo-distributions, while

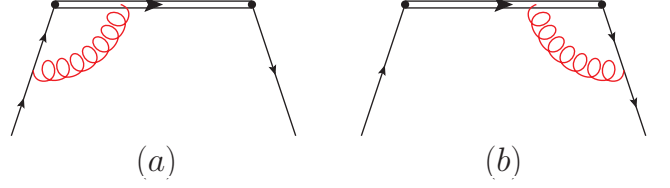


Figure 4: Vertex-like diagrams contribution.

the second contains the mass singularity plus a finite term. We observe that, besides the dominant logarithmic behaviour, accounting for mass effects in the pseudo-distribution leads to a resummation of higher-twist contributions proportional to powers of $z^2 m^2$.¹ Finally, the term proportional to $K_1(\sqrt{-z^2(1-\beta)^2 m^2})$ in the fifth and sixth lines of eq. (28) is the combination of both finite-mass and off-light-cone effects. At leading twist, it has no-dependence on z^2 , as expected.

We verified that, in the massless limit, our calculation reproduces the expected result. It is important to note that this comparison cannot be done naively starting from the final result of the diagram and performing an expansion for $z^2 m^2 \rightarrow 0$. The correct result is obtained by setting to zero all mass-related terms from the start. The resulting integrals can then be computed in dimensional regularisation with $D \neq 4$. We do not present here the comparison diagram by diagram, but directly show the consistency between massive and massless calculations for the full one-loop distribution.

3.4. Vertex-type contribution

The vertex correction is associated to the two diagrams in fig. 4. The contribution of these two diagrams to the forward matrix element is the same, therefore we consider only (b) and include (a) by multiplying the result by a factor of two. At the operator level, we have

$$\mathcal{O}_{\text{Vertex,b}}^\alpha = g^2 C_F \int_0^1 dt \int d^D z_1 \times D_{\mu\nu}(z_1 - zt) \bar{\psi}(z_1) \gamma^\mu D_F(z_1) \gamma^\alpha \psi(z) z^\nu. \quad (30)$$

Moving to the quark distribution, we obtain

$$\begin{aligned} \mathcal{M}_{\text{Vertex,b}}(\nu, z^2, m^2) &= -\frac{g^2 C_F}{2} \frac{\Gamma\left(\frac{D}{2} - 1\right)}{(4\pi)^{D/2}} i e^{i\nu} \sum_\lambda \int_0^1 dt \int d^D z_1 \\ & \quad \times \int \frac{d^D k}{(2\pi)^D} \frac{e^{i(p-k)z_1}}{[-(z_1 - zt)^2/4 + i0]^{D/2-1}} \\ & \quad \times \bar{u}_\lambda(p) \not{t} \frac{\not{k} + m}{k^2 - m^2 + i0} \gamma^\alpha u_\lambda(p). \quad (31) \end{aligned}$$

¹Each of these power terms also contains a $\ln(-z^2)$ term according to the standard form of the operator product expansion.

Performing the shift $z_1 \rightarrow z_1 + zt$ and using the integral in eq. (26), we get

$$\mathcal{M}_{\text{Vertex,b}}(\nu, z^2, m^2) = \frac{g^2 C_F}{2} \int_0^1 dt e^{i\nu(1-t)} \times \int \frac{d^D k}{(2\pi)^D} \frac{e^{-ik \cdot zt} \text{Tr} [t k \gamma^0 \not{p}]}{[(k-p)^2 + i0][k^2 - m^2 + i0]}, \quad (32)$$

where we implicitly used the choice $z = (0, 0, 0, z^3)$. The vertex correction is the most complex and thus we again postpone the detailed derivation of the result to a future publication [45].

The complete result for the vertex contribution reads

$$\begin{aligned} & \mathcal{M}_{\text{Vertex}}(\nu, z^2, m^2) \\ &= -\frac{g^2 C_F}{(4\pi)^{D/2}} \frac{2\Gamma\left(\frac{D}{2} - 1\right)}{\left(\frac{D}{2} - 2\right)} \left(\frac{-z^2}{4}\right)^{2-D/2} \mathcal{M}^0(\nu) \\ &+ \frac{2g^2 C_F}{(4\pi)^{D/2}} \int_0^1 d\beta \left[\frac{4\beta}{1-\beta} K_0\left(\sqrt{-z^2(1-\beta)^2 m^2}\right) \right]_+ \mathcal{M}^0(\beta\nu) \\ &- \frac{2g^2 C_F}{(4\pi)^{D/2}} \int_0^1 d\beta \left[4\Phi(1-\beta, \sqrt{-z^2 m^2}) \mathcal{M}^0(\beta\nu) \right. \\ &- 4\left(\frac{\ln(1-\beta) + \beta}{1-\beta}\right) \mathcal{M}^0(\nu) \left. \right] - \frac{4g^2 C_F}{(4\pi)^D} \mathcal{M}^0(\nu) R(\sqrt{-z^2 m^2}) \\ &+ \frac{g^2 C_F}{(4\pi)^{D/2}} \int_0^1 d\beta \left[\frac{4\beta}{1-\beta} \right]_+ \mathcal{M}^0(\beta\nu) \\ &\times \sqrt{-z^2(1-\beta)^2 m^2} K_1\left(\sqrt{-z^2(1-\beta)^2 m^2}\right), \quad (33) \end{aligned}$$

where

$$\begin{aligned} & \Phi(1-\beta, \sqrt{-z^2 m^2}) \\ &\equiv \int_{1-\beta}^1 dt \frac{\partial}{\partial \beta} \left[\left(\frac{1-\beta}{t^2} - \frac{1}{t} \right) \right. \\ &\times \left. \left[K_0\left(\sqrt{-z^2 m^2(1-\beta)^2}\right) - K_0\left(\frac{\sqrt{-z^2 m^2(1-\beta)^2}}{t}\right) \right] \right] \\ &= \frac{\ln(1-\beta) + \beta}{1-\beta} + \mathcal{O}(-z^2 m^2) \quad (34) \end{aligned}$$

and

$$\begin{aligned} R(\sqrt{-z^2 m^2}) &= \lim_{\beta \rightarrow 1} \int_{1-\beta}^1 \frac{dt}{t} \left(1 - \frac{1-\beta}{t} \right) \left[K_0\left(\sqrt{-z^2 m^2(1-\beta)}\right) \right. \\ &\left. - K_0\left(\frac{\sqrt{-z^2 m^2(1-\beta)}}{t}\right) + \ln t \right]. \quad (35) \end{aligned}$$

The UV-divergent term in the second line of eq. (33) is identical to the massless case. The term proportional to $K_0\left(\sqrt{-z^2(1-\beta)^2 m^2}\right)$ generalises the z^2 -evolution term of the massless case. Indeed, when combined with an analogous term in the box-type correction, it produces the expected structure

$$\left[\frac{1+\beta^2}{1-\beta} K_0\left(\sqrt{-z^2(1-\beta)^2 m^2}\right) \right]_+. \quad (36)$$

The term proportional to $K_1\left(\sqrt{-z^2(1-\beta)^2 m^2}\right)$ exactly cancels against the box and, in the leading-twist approximation, it is the *UV-finite term* of Ref. [21]. More complications arise from the fourth and fifth line of eq. (33). A first important remark is that the integrand in β is finite when $\beta \rightarrow 1$. Indeed, the function $\Phi(1-\beta, \sqrt{-z^2 m^2})$ is singular for $\beta = 1$ and its expansion around this value gives

$$\Phi(1-\beta, \sqrt{-z^2 m^2}) = \frac{\beta + \ln(1-\beta)}{1-\beta} + \mathcal{O}((1-\beta)^0). \quad (37)$$

Thus, the whole square bracket involving the Φ function in eq. (33) is regular at $\beta = 1$. Also, in the leading-twist approximation ($z^2 m^2 \rightarrow 0$), this term reduces to the so-called *IR-finite term* of Ref. [21]. The function $R(\sqrt{-z^2 m^2})$ in the fifth line of eq. (33) is finite and of $\mathcal{O}(-z^2 m^2)$ (thus absent in the massless limit). One may insist on computing R in a closed form. However, it turned out to be easier to evaluate it numerically. Moreover, in the pseudo-distribution approach, its exact form is unimportant, since it cancels when taking the *reduced* Ioffe-time distribution [21].

Finally, we checked the consistency with the massless limit also for this contribution.

3.5. Off-light-cone distribution at one-loop

The complete massive Ioffe-time distribution is obtained by combining eqs. (16), (22), (28), and (33). We find²

$$\begin{aligned} & \mathcal{M}^{1\text{-loop}}(\nu, z^2, m^2) \\ &= \frac{2g^2 C_F}{(4\pi)^{D/2}} \left\{ Z(z^2) \mathcal{M}^0(\nu) \right. \\ &+ \int_0^1 d\beta \left[\frac{1+\beta^2}{1-\beta} 2K_0\left(\sqrt{-z^2(1-\beta)^2 m^2}\right) - 4\frac{\ln(1-\beta) + \beta}{1-\beta} \right]_+ \mathcal{M}^0(\beta\nu) \\ &\left. - 4 \int_0^1 d\beta \left[\Phi(1-\beta, \sqrt{-z^2 m^2}) - \left(\frac{\ln(1-\beta) + \beta}{1-\beta} \right) \right] \mathcal{M}^0(\beta\nu) \right\}, \quad (38) \end{aligned}$$

where the function

$$\begin{aligned} Z(z^2) &= -\frac{(D-1)}{(D-4)(D-3)} \left(\frac{-z^2}{4e^{-\gamma_E}} \right)^{2-D/2} \\ &+ 2 \left[\frac{1 - \sqrt{-z^2 m^2} K_1\left(\sqrt{-z^2 m^2}\right)}{-z^2 m^2} + \frac{1}{4} \ln\left(\frac{-z^2 m^2}{4e^{-2\gamma_E}}\right) - R(\sqrt{-z^2 m^2}) \right] \quad (39) \end{aligned}$$

collects the (divergent) terms that drop when considering the reduced Ioffe-time distribution [21].

4. Matching kernel

Before building the massive matching kernel, we inspect the leading term in the $z^2 m^2 \rightarrow 0$ limit, to show the consistency

²Note that we added and subtracted a suitable contribution to isolate the higher-twist part of the function Φ in the last line of eq. (38).

with the massless computation. We multiply eq. (38) by a factor

$$S_D = \frac{(e^{\gamma_E})^{2-D/2}}{(4\pi)^{2-D/2}} \quad (40)$$

to implement the $\overline{\text{MS}}$ scheme and consider only the leading term in the expansion around $z^2 m^2 = 0$, obtaining

$$\begin{aligned} & \mathcal{M}^{1\text{-loop}}(v, z^2, m^2) \Big|_{z^2 m^2 \rightarrow 0} \\ &= -\frac{\bar{g}^2 C_F}{8\pi^2} \left\{ \int_0^1 d\beta \left[\frac{1+\beta^2}{1-\beta} \left(\ln \left(\frac{-z^2 m^2}{4e^{-2\gamma_E}} \right) + 2 \ln(1-\beta) + 1 \right) \right] \right. \\ & \quad \times \mathcal{M}^0(\beta v) + \int_0^1 d\beta \left[\frac{4 \ln(1-\beta)}{1-\beta} - 2(1-\beta) \right]_+ \mathcal{M}^0(\beta v) \\ & \quad \left. - \tilde{Z}(z^2) \mathcal{M}^0(v) \right\}, \quad (41) \end{aligned}$$

where $g = \bar{g}\mu^\epsilon$ and

$$\tilde{Z}(z^2) = Z(z^2) \Big|_{z^2 m^2 \rightarrow 0} = \frac{3}{2} \left(\frac{1}{\epsilon_{\text{UV}}} + \ln \left(\frac{-z^2 \mu^2}{4e^{-2\gamma_E}} \right) \right) + \frac{5}{2}. \quad (42)$$

The massive pseudo-distribution, expanded for $z^2 m^2 \rightarrow 0$, is almost identical to the massless one, which, adopting dimensional regularisation also for the IR-sector,³ reads

$$\begin{aligned} & \mathcal{M}^{1\text{-loop}}(v, z^2, 0) \\ &= -\frac{\bar{g}^2 C_F}{8\pi^2} \left\{ \int_0^1 d\beta \left[\frac{1+\beta^2}{1-\beta} \left(\ln \left(\frac{-z^2 \mu^2}{4e^{-2\gamma_E}} \right) + \frac{1}{\epsilon_{\text{IR}}} \right) \right] \right. \\ & \quad \left. + \int_0^1 d\beta \left[\frac{4 \ln(1-\beta)}{1-\beta} - 2(1-\beta) \right]_+ \mathcal{M}^0(\beta v) - \tilde{Z}(z^2) \mathcal{M}^0(v) \right\}. \quad (43) \end{aligned}$$

Both distributions in eqs. (41) and (43) are now renormalised in the $\overline{\text{MS}}$ scheme by simply removing the UV-pole in $\tilde{Z}(z^2)$. It is clear that, in the massive case, the infrared pole is replaced by the logarithm of the mass and a finite term proportional to $(2 \ln(1-\beta) + 1)$ appeared.

This difference between the two Ioffe-time distributions is actually correct. Indeed, while the massless Ioffe-time distribution must be matched onto the massless light-cone Ioffe-time distribution

$$\mathcal{I}^{1\text{-loop}}(v, \mu^2, 0) = \frac{\bar{g}^2}{8\pi^2} C_F \int_0^1 d\beta \left[\frac{1+\beta^2}{1-\beta} \right]_+ \left(\frac{1}{\epsilon_{\text{UV}}} - \frac{1}{\epsilon_{\text{IR}}} \right) \mathcal{M}^{(0)}(\beta v), \quad (44)$$

the massive version must be matched onto the massive generalisation of eq. (44), which reads

$$\begin{aligned} \mathcal{I}^{1\text{-loop}}(v, \mu^2, m^2) &= \frac{\bar{g}^2}{8\pi^2} C_F \int_0^1 d\beta \mathcal{M}^0(\beta v) \\ & \quad \times \left[\frac{1+\beta^2}{1-\beta} \left(\frac{1}{\epsilon_{\text{UV}}} - \ln \left(\frac{m^2}{\mu^2} \right) - 2 \ln(1-\beta) - 1 \right) \right]_+. \quad (45) \end{aligned}$$

We observe that in eq. (45), in addition to the UV-pole, we have the term

$$\left[\frac{1+\beta^2}{1-\beta} \left(-\ln \left(\frac{m^2}{\mu^2} \right) - 2 \ln(1-\beta) - 1 \right) \right]_+, \quad (46)$$

which is a known result in the context of the so-called heavy-quark threshold matching relevant for PDF evolution in a variable-flavour-number scheme [46].

As it can be seen by comparing eqs. (41) and (45) with eqs. (43) and (44), at the level of the leading term in the $z^2 m^2 \rightarrow 0$ limit (*i.e.* the leading-twist approximation), the massive matching kernel is the same as in the massless case. The difference is therefore that the former accounts for higher-power corrections of the type $z^2 m^2$, incorporated in the Bessel functions.

After these premises, we can build the complete matching of eq. (38) (consistently renormalised in the $\overline{\text{MS}}$ scheme) on eq. (45) and obtain

$$\begin{aligned} & \mathcal{M}^{1\text{-loop}}(v, z^2, m^2) \\ &= \mathcal{I}^{1\text{-loop}}(v, \mu^2, m^2) + \frac{\bar{g}^2 C_F}{8\pi^2} \left\{ Z_{\text{R}}(z^2) \mathcal{I}^0(v) \right. \\ & \quad + \int_0^1 d\beta \left[\frac{1+\beta^2}{1-\beta} \left(2K_0 \left(\sqrt{-z^2(1-\beta)^2 m^2} \right) \right. \right. \\ & \quad \left. \left. + \ln \left(\frac{m^2}{\mu^2} \right) + 2 \ln(1-\beta) + 1 \right) - 4 \frac{\ln(1-\beta) + \beta}{1-\beta} \right]_+ \mathcal{I}^0(\beta v) \\ & \quad \left. - 4 \int_0^1 d\beta \left[\Phi(1-\beta, \sqrt{-z^2 m^2}) - \left(\frac{\ln(1-\beta) + \beta}{1-\beta} \right) \right] \mathcal{I}^0(\beta v) \right\}, \quad (47) \end{aligned}$$

where

$$\begin{aligned} Z_{\text{R}}(z^2) &= 2 + \frac{3}{2} \ln \left(\frac{-z^2 \mu^2}{4e^{-\gamma_E}} \right) + 2 \left[\frac{1 - \sqrt{-z^2 m^2} K_1 \left(\sqrt{-z^2 m^2} \right)}{-z^2 m^2} \right. \\ & \quad \left. + \frac{1}{4} \ln \left(\frac{-z^2 m^2}{4e^{-2\gamma_E}} \right) - R \left(\sqrt{-z^2 m^2} \right) \right]. \quad (48) \end{aligned}$$

5. Numerical analysis

In order to estimate quantitatively the effect of heavy-quark mass corrections on pseudo-distributions, we consider a proton target and write the matching between the off-light-cone and light-cone parton distributions in a factorised form as follows:

$$f(x, z^2, \mu^2) = \int_x^1 \frac{dy}{y} C(y, z^2 \mu^2, z^2 m^2, g) f \left(\frac{x}{y}, 0, \mu^2 \right), \quad (49)$$

where, up to one-loop accuracy,

$$\begin{aligned} & C(y, z^2 \mu^2, z^2 m^2, \bar{g}) \\ &= \delta(1-y) + \frac{\bar{g}^2}{8\pi^2} \left\{ Z_{\text{R}}(z^2) \delta(1-y) + \left[\frac{1+y^2}{1-y} \left(2K_0 \left(\sqrt{-z^2 m^2(1-y)^2} \right) \right. \right. \right. \\ & \quad \left. \left. + \ln \left(\frac{m^2}{\mu^2} \right) + 2 \ln(1-y) + 1 \right) - 4 \frac{\ln(1-y) + y}{1-y} \right]_+ \\ & \quad \left. - 4 \left(\Phi \left(1-y, \sqrt{-z^2 m^2} \right) - \frac{\ln(1-y) + y}{1-y} \right) \right\}. \quad (50) \end{aligned}$$

³For simplicity, we adopt a unique scale μ .

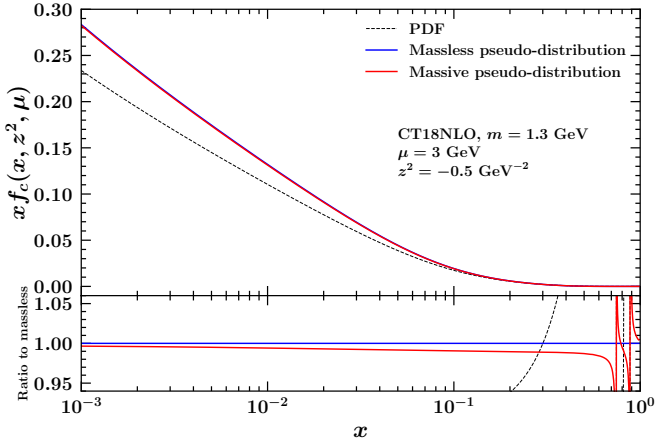


Figure 5: Charm-quark pseudo distribution as a function of the longitudinal momentum fraction x computed by means of eq. (49).

In fig. 5, we computed the charm pseudo-distribution of the proton obtained by means of eq. (49). In the computation, we used the charm PDF (and the running of the strong coupling) from the CT18NLO set [47], accessed through the LHAPDF interface [48]. We set $\mu = 3$ GeV, $m = 1.3$ GeV, and $z^2 = -0.5$ GeV⁻². The upper panel of the plot shows the charm light-cone PDF (dashed curve), the charm pseudo-distribution in the massless limit (red solid curve), and the massive charm pseudo-distribution (blue solid curve). The lower panel, displays the same curves normalised to the massless calculation. Comparing massive and massless curves, we find that the effect of heavy-quark mass corrections is remarkably small, of the order of a few percent. We also verified that a similar magnitude of differences is found for other kinematic configurations. This observation indicates that there is a strong and unexpected suppression of power corrections of the form $z^2 m^2$ which requires further investigations. We leave a detailed quantitative study of this phenomenon to a future publication [45].

6. Summary and conclusions

We have computed the one-loop correction to the forward matrix element of an off-light-cone bi-local quark correlator, often referred to as pseudo-distribution, accounting for heavy-quarks mass effects. This calculation allowed us to extract the non-singlet matching kernel on the corresponding PDF.

The computation is performed in Feynman gauge and features four contributions: the Wilson-line self-energy (sec. 3.1), the quark-line self-energy (sec. 3.2), the box-type contribution (sec. 3.3), and the vertex-type contribution (sec. 3.4). The latter contribution turned out to be the most challenging to compute. Indeed, the function Φ , introduced in eq. (3.4) in a semi-analytical fashion, is affected by a non-integrable end-point singularity that needs to be treated with care. We proved that this singularity cancels in the final result and made the cancellation apparent by expressing the vertex-type contribution in a manifestly convergent form. The final result, presented in eq. (47), resums all powers of $z^2 m^2$ by means of modified Bessel func-

tions of the second kind up to one-loop perturbative accuracy. We also noted that when constructing the *reduced* Ioffe-time distribution the Z_R cancels out.

In order to assess the quantitative impact of mass effects, we carried out a numerical implementation of our result. After having extracted the matching function appropriate to construct the pseudo-distribution in terms of the PDF, we evaluated the charm pseudo-distribution in the proton using both our massive calculation and the known massless calculation. When comparing the two results, we found that the impact of the quark-mass corrections is remarkably small and is around the percent level. This result suggests that the use of the massless matching kernel adopted in previous studies on heavy mesons [38–40] is more accurate than expected. However, in a forthcoming publication, we will investigate this finding more in depth. Specifically, we will compute one-loop mass corrections also in the singlet sector by considering gluon external states and assess their numerical impact. We will also take the opportunity to provide additional computational details of the calculation presented in this paper.

Acknowledgements

We are grateful to Benoît Blossier, Teseo San José, José Manuel Morgado Chávez, Alessandro Papa, Simone Rodini, Samuel Wallon, and Lech Szymanowski for fruitful discussions. The work of M.F. is supported by the Agence Nationale de la Recherche under the contract ANR-17-CE31-0019. M.F. acknowledges support from the Italian Foundation “Angelo Della Riccia”. The work of CM is supported, in part, by l’Agence Nationale de la Recherche (ANR), project ANR-23-CE31-0019. This work was made possible by Institut Pascal at Université Paris-Saclay with the support of the program “Investissements d’avenir” ANR-11-IDEX-0003-01. For the purpose of open access, the authors have applied a CC-BY public copyright licence to any Author Accepted Manuscript (AAM) version arising from this submission. Feynman diagrams have been drawn using JaxoDraw [49].

References

- [1] Krzysztof Cichy and Martha Constantinou. A guide to light-cone PDFs from Lattice QCD: an overview of approaches, techniques and results. *Adv. High Energy Phys.*, 2019:3036904, 2019.
- [2] A. V. Radyushkin. Theory and applications of parton pseudodistributions. *Int. J. Mod. Phys. A*, 35(05):2030002, 2020.
- [3] Martha Constantinou et al. Parton distributions and lattice-QCD calculations: Toward 3D structure. *Prog. Part. Nucl. Phys.*, 121:103908, 2021.
- [4] Keh-Fei Liu and Shao-Jing Dong. Origin of difference between anti-d and anti-u partons in the nucleon. *Phys. Rev. Lett.*, 72:1790–1793, 1994.
- [5] William Detmold and C. J. David Lin. Deep-inelastic scattering and the operator product expansion in lattice QCD. *Phys. Rev. D*, 73:014501, 2006.
- [6] V. Braun and Dieter Müller. Exclusive processes in position space and the pion distribution amplitude. *Eur. Phys. J. C*, 55:349–361, 2008.
- [7] Xiangdong Ji. Parton Physics on a Euclidean Lattice. *Phys. Rev. Lett.*, 110:262002, 2013.
- [8] A. V. Radyushkin. Quasi-parton distribution functions, momentum distributions, and pseudo-parton distribution functions. *Phys. Rev. D*, 96(3):034025, 2017.

- [9] A. J. Chambers, R. Horsley, Y. Nakamura, H. Perlt, P. E. L. Rakow, G. Schierholz, A. Schiller, K. Somfleth, R. D. Young, and J. M. Zanotti. Nucleon Structure Functions from Operator Product Expansion on the Lattice. *Phys. Rev. Lett.*, 118(24):242001, 2017.
- [10] Yan-Qing Ma and Jian-Wei Qiu. Exploring Partonic Structure of Hadrons Using ab initio Lattice QCD Calculations. *Phys. Rev. Lett.*, 120(2):022003, 2018.
- [11] Gunnar S. Bali, Peter C. Bruns, Luca Castagnini, Markus Diehl, Jonathan R. Gaunt, Benjamin Gläsel, Andreas Schäfer, André Sternbeck, and Christian Zimmermann. Two-current correlations in the pion on the lattice. *JHEP*, 12:061, 2018.
- [12] Andrea Shindler. Moments of parton distribution functions of any order from lattice QCD. *Phys. Rev. D*, 110(5):L051503, 2024.
- [13] Xiaonu Xiong, Xiangdong Ji, Jian-Hui Zhang, and Yong Zhao. One-loop matching for parton distributions: Nonsinglet case. *Phys. Rev. D*, 90(1):014051, 2014.
- [14] Xiangdong Ji, Peng Sun, Xiaonu Xiong, and Feng Yuan. Soft factor subtraction and transverse momentum dependent parton distributions on the lattice. *Phys. Rev. D*, 91:074009, 2015.
- [15] Xiangdong Ji, Andreas Schäfer, Xiaonu Xiong, and Jian-Hui Zhang. One-Loop Matching for Generalized Parton Distributions. *Phys. Rev. D*, 92:014039, 2015.
- [16] Anatoly Radyushkin. Nonperturbative Evolution of Parton Quasi-Distributions. *Phys. Lett. B*, 767:314–320, 2017.
- [17] A. V. Radyushkin. Structure of parton quasi-distributions and their moments. *Phys. Lett. B*, 788:380–387, 2019.
- [18] Long-Bin Chen, Wei Wang, and Ruilin Zhu. Master integrals for two-loop QCD corrections to quark quasi PDFs. *JHEP*, 10:079, 2020.
- [19] Long-Bin Chen, Wei Wang, and Ruilin Zhu. Next-to-Next-to-Leading Order Calculation of Quasiparton Distribution Functions. *Phys. Rev. Lett.*, 126(7):072002, 2021.
- [20] Anatoly Radyushkin. One-loop evolution of parton pseudo-distribution functions on the lattice. *Phys. Rev. D*, 98(1):014019, 2018.
- [21] A. V. Radyushkin. Quark pseudodistributions at short distances. *Phys. Lett. B*, 781:433–442, 2018.
- [22] Anatoly V. Radyushkin. Generalized parton distributions and pseudodistributions. *Phys. Rev. D*, 100(11):116011, 2019.
- [23] Ian Balitsky, Wayne Morris, and Anatoly Radyushkin. Gluon Pseudo-Distributions at Short Distances: Forward Case. *Phys. Lett. B*, 808:135621, 2020.
- [24] Ian Balitsky, Wayne Morris, and Anatoly Radyushkin. Polarized gluon pseudodistributions at short distances. *JHEP*, 02:193, 2022.
- [25] Ian Balitsky, Wayne Morris, and Anatoly Radyushkin. Short-distance structure of unpolarized gluon pseudodistributions. *Phys. Rev. D*, 105(1):014008, 2022.
- [26] Fei Yao, Yao Ji, and Jian-Hui Zhang. Connecting Euclidean to light-cone correlations: from flavor nonsinglet in forward kinematics to flavor singlet in non-forward kinematics. *JHEP*, 11:021, 2023.
- [27] Anatoly Radyushkin. Target Mass Effects in Parton Quasi-Distributions. *Phys. Lett. B*, 770:514–522, 2017.
- [28] Vladimir M. Braun, Yao Ji, and Alexey Vladimirov. QCD factorization for chiral-odd parton quasi- and pseudo-distributions. *JHEP*, 10:087, 2021.
- [29] Vladimir M. Braun, Yao Ji, and Alexey Vladimirov. QCD factorization for twist-three axial-vector parton quasidistributions. *JHEP*, 05:086, 2021.
- [30] V. M. Braun. Kinematic twist-three contributions to pseudo- and quasi-GPDs and translation invariance. *JHEP*, 10:134, 2023.
- [31] Vladimir M. Braun, Maria Koller, and Jakob Schoenleber. Renormalons and power corrections in pseudo- and quasi-GPDs. *Phys. Rev. D*, 109(7):074510, 2024.
- [32] Chao Han, Wei Wang, Jia-Lu Zhang, and Jian-Hui Zhang. Power corrections to quasidistribution amplitudes of a heavy meson. *Phys. Rev. D*, 110(9):094038, 2024.
- [33] Shohini Bhattacharya, Krzysztof Cichy, Martha Constantinou, Andreas Metz, Niilo Nurminen, and Fernanda Steffens. Generalized parton distributions from the pseudodistribution approach on the lattice. *Phys. Rev. D*, 110(5):054502, 2024.
- [34] Hervé Dutrieux, Robert G. Edwards, Colin Egerer, Joseph Karpie, Christopher Monahan, Kostas Orginos, Anatoly Radyushkin, David Richards, Eloy Romero, and Savvas Zafeiropoulos. Towards unpolarized GPDs from pseudo-distributions. *JHEP*, 08:162, 2024.
- [35] Michael Joseph Riberdy, Hervé Dutrieux, Cédric Mezrag, and Paweł Sznajder. Combining lattice QCD and phenomenological inputs on generalised parton distributions at moderate skewness. *Eur. Phys. J. C*, 84(2):201, 2024.
- [36] J. Karpie, R. M. Whitehill, W. Melnitchouk, C. Monahan, K. Orginos, J. W. Qiu, D. G. Richards, N. Sato, and S. Zafeiropoulos. Gluon helicity from global analysis of experimental data and lattice QCD Ioffe time distributions. *Phys. Rev. D*, 109(3):036031, 2024.
- [37] Krzysztof Cichy, Martha Constantinou, Paweł Sznajder, and Jakub Wagner. Nucleon tomography and total angular momentum of valence quarks from synergy between lattice QCD and elastic scattering data. 9 2024.
- [38] Shuai Zhao and Anatoly V. Radyushkin. B -meson Ioffe-time distribution amplitude at short distances. *Phys. Rev. D*, 103(5):054022, 2021.
- [39] Benoît Blossier, Mariane Mangin-Brinet, José Manuel Morgado Chávez, and Tesco San José. The distribution amplitude of the η_c -meson at leading twist from lattice QCD. *JHEP*, 09:079, 2024.
- [40] B. Blossier, C. Mezrag, J. M. Morgado Chávez, and T. San José. Lattice QCD extraction of the η_c -meson t -dependent parton distribution function. In *31st International Workshop on Deep-Inelastic Scattering and Related Subjects*, 9 2024.
- [41] Pavel M. Nadolsky, Nikolaos Kidonakis, F. I. Olness, and C. P. Yuan. Resummation of transverse momentum and mass logarithms in DIS heavy quark production. *Phys. Rev. D*, 67:074015, 2003.
- [42] Rebecca von Kuk, Johannes K. L. Michel, and Zhiqian Sun. Transverse momentum distributions of heavy hadrons and polarized heavy quarks. *JHEP*, 09:205, 2023.
- [43] I. I. Balitsky and Vladimir M. Braun. Evolution Equations for QCD String Operators. *Nucl. Phys. B*, 311:541–584, 1989.
- [44] John Collins. Foundations of perturbative QCD. *Camb. Monogr. Part. Phys. Nucl. Phys. Cosmol.*, 32:1–624, 2011.
- [45] V. Bertone, M. Fucilla, and C. Mezrag. to appear. 2025.
- [46] Richard D. Ball, Valerio Bertone, Marco Bonvini, Stefano Forte, Patrick Groth Merrild, Juan Rojo, and Luca Rottoli. Intrinsic charm in a matched general-mass scheme. *Phys. Lett. B*, 754:49–58, 2016.
- [47] Tie-Jiun Hou et al. New CTEQ global analysis of quantum chromodynamics with high-precision data from the LHC. *Phys. Rev. D*, 103(1):014013, 2021.
- [48] Andy Buckley, James Ferrando, Stephen Lloyd, Karl Nordström, Ben Page, Martin Rüfenacht, Marek Schönherr, and Graeme Watt. LHAPDF6: parton density access in the LHC precision era. *Eur. Phys. J. C*, 75:132, 2015.
- [49] D. Binosi, J. Collins, C. Kaufhold, and L. Theussl. JaxoDraw: A Graphical user interface for drawing Feynman diagrams. Version 2.0 release notes. *Comput. Phys. Commun.*, 180:1709–1715, 2009.